

**The Design of Lipid Nanoparticles for Delivery of RNA Therapeutics as a Treatment for  
Acute Myeloid Leukemia**

A Technical Report submitted to the Department of Biomedical Engineering

Presented to the Faculty of the School of Engineering and Applied Science  
University of Virginia • Charlottesville, Virginia

In Partial Fulfillment of the Requirements for the Degree  
Bachelor of Science, School of Engineering

**Colin Haws**

Spring, 2022

On my honor as a University Student, I have neither given nor received unauthorized aid on this  
assignment as defined by the Honor Guidelines for Thesis-Related Assignments

Dr. Anuradha Illendula, Department of Pharmacology

# The Design of Lipid Nanoparticles for Delivery of RNA Therapeutics as a Treatment for Acute Myeloid Leukemia

Colin C. Haws

<sup>a</sup> Department of Biomedical Engineering, University of Virginia

<sup>1</sup> Correspondence: cch3mf@virginia.edu

## Abstract

Acute myeloid leukemia (AML) is a rare disease characterized by the overproduction of immature white blood cells which lead to infections and a poor survival rate. The current standard of care for treating AML, chemotherapies, are rendered ineffective due to genome-specific mechanisms of drug resistance. The proposed therapy investigates the knockdown of nuclear-related factor 2 (Nrf2), a transcription factor known to propagate AML cell survival through antioxidant pathways. This therapeutic strategy was employed through scalable lipid nanoparticle (LNP) formulation encapsulating anti-Nrf2 small interfering ribonucleic acid (siRNA) to increase the potency of chemotherapies in AML patients. Physiologically viable, monodispersed siRNA-LNPs were formulated with size below 200 nanometers and PDI less than 0.125. These particles demonstrated efficient transfection of suspension AML cell lines through incorporation of a lipid dye and a 2.51-fold Nrf2 mRNA knockdown in KG1 cells. Preliminary *in vitro* cell viability data over a 4-day window demonstrate potential for the anti-Nrf2 siRNA LNP design as a novel combinatorial therapy with cytarabine. Future studies will investigate the versatility of transfection through treatment of primary AML cell cultures as well as the incorporation of CD molecules for heightened LNP targeting. Present findings utilizing a highly scalable formulation design present a viable treatment alternative with clinical applications to AML and several other genetically induced diseases.

Keywords: Lipid nanoparticles (LNPs), small interfering ribonucleic acid (siRNA), nuclear-related factor 2 (Nrf2)

---

## Introduction

Acute myeloid leukemia (AML) is a cancer originating in the bone marrow characterized by a rapid accumulation of immature white blood cells. This period of uncontrolled cell growth puts patients at increased risk of infection and is characterized by a five-year survival rate of 26% as well as a near 50% rate of relapse<sup>1-3</sup>. Patients with AML are conventionally treated with chemotherapies which rely on an oxidative stress pathway to induce cell death. Immunotherapies such as chimeric antigen receptor T-cell therapy and transplant avenues using stem cells remain in early stages of research or are limited to AML patients with selective biomarkers. Therefore, a treatment vector to be combined with the chemotherapeutic standard of care may have the most immediate possibility of clinical translation. This sentiment has spurred several researchers to investigate avenues for improving the efficiency of chemotherapies. Central to this challenge is the development of chemoresistance in AML cell lines. This mechanism has been elucidated in literature to occur

through the nuclear-related factor 2 (Nrf2) activated pathway which decreases cytotoxic effects of reactive oxygen species (ROS) through transcriptional regulation<sup>4,5</sup>. Nrf2 has therefore become a popular genetic target for treating a host of cancer subtypes.

Previous studies have demonstrated the suppression of Nrf2 triggers ROS-induced cell death in a tumor microenvironment<sup>6,7</sup>. However, the clinical translation of these approaches are limited by several factors including poor drug solubility, pharmacokinetics, and off-target effects. A recent study discovered an effective inhibitor termed K67 which induces Nrf2 degradation and increases local cytotoxicity when paired with chemotherapeutics. However, K67 presents low solubility in appropriate solutions, requiring compound functional group modification or particle encapsulation for therapeutic value<sup>8</sup>. This issue has been addressed through encapsulation of similar drugs into nanoparticles most commonly composed of polymers or lipids. The use of these vectors circumvents prior issues of drug solubility

and pharmacokinetics through particle component modulation. Particles may be designed in ratios of varying hydrophobic character or charge-charge interactions to heighten encapsulation and delivery to clinically acceptable metrics. Though nanoscale formulations have revolutionized drug delivery, off-target effects intrinsic to the drug itself continue to restrict these therapies from reaching patients.

In AML patients, regimented treatments are delivered either orally or intravenously. These processes demonstrate relatively noninvasive measures but leads to systemic delivery. In the scope of a similarly delivered Nrf2 inhibitor, current combinatorial treatments lead to off-target effects creating cytotoxic environments in healthy tissues. This effect was observed in literature with the delivery of plumbagin, a molecule which inhibits Nrf2 translocation to the nucleus. Upon liposome encapsulation, a prolonged delivery of plumbagin to cancer cells in vitro led to favorable cytotoxicity. However, when these experiments are recapitulated in vivo, off-target effects induce toxicity in the liver and other healthy tissues through molecular binding mechanisms which remain to be elucidated<sup>6,9</sup>. Conjugation of additional elements into nanoparticle complexes such as liposomes have partially addressed this problem through cell specific targeting but these approaches are rarely reproducible on a large scale due to the necessity of several characterization processes following time-intensive processes<sup>10</sup>. An alternative to this approach utilizes delivery of siRNAs which inherently eliminate off-target effects by inducing mRNA cleavage based on stringent, base pair binding. This process has been vindicated on a small scale utilizing LNPs to transfect leukemic cell lines with encapsulated siRNA as a proof of concept<sup>11</sup>. It should be noted the use of LNPs in this application is preferred to polymer-based formulations based on previous clinical success of Patisiran, a lipid based complex used as a treatment for polyneuropathy of hereditary transthyretin-mediated amyloidosis<sup>12</sup>.

The proposed project investigates the efficiency of lipid-based siRNA therapeutic synthesis using high-throughput microfluidics. The design builds off previous successes in Nrf2 targeting and LNP formulation to introduce a novel combinational therapy for patients with AML. **Through adaptation of technologies which directly address current pitfalls in AML treatment research, this approach offers a specialized vector to prevent**

**chemoresistance in AML patients with opportunity for large scale manufacturing to aid in clinical translation.**

### Project Aims

#### *Aim I: Formulate monodispersed anti-Nrf2 siRNA LNPs*

Previous studies used high-throughput microfluidics to optimize lipid molar ratios for heightened siRNA encapsulation and ideal size characteristics<sup>13-15</sup>. As these lipids are mechanistically responsible for RNA encapsulation, the proposed formulation is theorized to achieve similar siRNA encapsulation metrics. Nanoparticle size and zeta potential distributions will be analyzed in triplicate. These data will be averaged within test groups using the same microfluidic chip and benchtop parameters. If nanoparticle size distributions are polydisperse or consistently above 200 nm, formulations may be passed through a 220 um nucleopore filter. Estimations for lipid nanoparticle size were derived from liposomal carrier metrics (previous work with Dr. Anuradha Illendula) as well as research by van der Meel et. al.<sup>14</sup>. This work utilized the same microfluidic based approach for particle formulation as proposed here as well as the same instrumentation for characterization. Alternatively, component combinations may be optimized through Box-Behnken Design to interpolate optimal conditions for low particle diameter<sup>16</sup>. In the case of poor encapsulation, ultracentrifugation may be explored as an alternative to dialysis techniques for buffer exchange<sup>17</sup>. Further consultation with representatives from Precision Nanosystems and Dr. Sasha Klivanov will also aid in troubleshooting. **The optimized siRNA LNP vector will be characterized by an average particle size below 200 nm and a low magnitude, negative zeta potential.**

#### *Aim II: Design an effective siRNA template against Nrf2*

The principle of siRNA and base pair specific hybridization suggests high specificity in targeting Nrf2 mRNA. In reality, the siRNA design construct requires meticulous review to ensure no off-target binding within the genome as well as low probability of both heterodimerization (binding between siRNA molecules) and homodimerization (binding within siRNA molecules). These events may be discouraged through consultation of software which predict binding free energies. As all demonstrations are to be performed in silico using deterministic models, each sequence will be tested only once for homology and dimerization free energies. The proposed design metrics are based on previous research

and advice from Dr. Keith Kozminski. In the improbable situation of no discoverable sequences which fit the design criteria for homology and free energy estimation, construct selection will require further advice from Dr. Kozminski. **In order to validate an efficient siRNA design, a 21-nucleotide search of the siRNA must yield no results with higher than 80% sequence homology and dimerization free energies must have magnitudes less than 5 kilocalories.**

***Aim III: Discover a significant decrease in Nrf2 mRNA and protein production***

Before a combinatorial treatment may be tested, the LNP construct must be evaluated for its ability to knock down Nrf2 mRNA and protein expression. Quantification of Nrf2 transcripts and protein expression compared to a GAPDH housekeeping control will vindicate the siRNA designs from Aim II *in vitro*. Nrf2 mRNA and protein knockdown following siRNA delivery has previously been reported by Rushworth et. al. which grants a preliminary expectation of knockdown for the proposed work. mRNA and protein expression experiments are to be done in triplicate and standardized with housekeeping gene changes (assumes normality). A Welch's t-test will be used to determine significance between Nrf2 levels at an alpha level of 0.05 following 24 hours of transfection. There is a possibility in these experiments a significant fold change is not observed. This may arise from possible mutations in primer binding regions or ineffective antibodies. These problems may be overcome by transducing low passage cell lines or relying solely on RT-qPCR results. Further troubleshooting will require input from PhD candidate Luke Vass for more efficient primer design and methodology assistance. **Through RT-PCR and western blot, the proposed construct is hypothesized to half Nrf2 mRNA expression and reduce Nrf2 protein expression by at least 30% following normalization with a housekeeping gene.**

***Aim IV: Measure a cytotoxic effect when construct used as combinatorial treatment***

To validate the design as a therapeutic, the siRNA LNP system will be used in combination with cytarabine treatment and tested for cell viability similar to prior work<sup>48</sup>. The number of cells in treated and untreated samples will be compared using a Welch's t-test at a 0.05 significance level. Measurements will be conducted in triplicate. The temporal window of chemoresistance may be difficult to predict. Viability measurements will

therefore be recorded at several time points so long as time and siRNA resources permit. **This assay will be hypothetically characterized by a significant reduction of AML cell count following treatment of the combined therapy when compared to just cytarabine, the current standard of care.**

The specified aims will validate the formulation of monodispersed LNPs (Aim 1) with high encapsulation efficiency of an effective siRNA design (Aim 2) to demonstrate significant decrease in Nrf2 expression (Aim 3) upon leukemic B cell transfection and demonstrate therapeutic value as a treatment vector when combined with cytarabine (Aim 4).

## **Materials and Methods**

### ***Materials***

All custom siRNA constructs were purchased as Custom Dicer-Substrate siRNA (DsiRNA) from Integrated DNA Technologies, Inc. (Iowa, USA). Ambion scramble siRNA constructs were purchased from ThermoFisher (Waltham, MA). The citrate buffer was prepared 1,2-distearoyl-sn-glycero-3-phosphocholine (DSPC), 1,2-Dimyristoyl-rac-glycero-3-methoxypolyethylene glycol-2000 (DMG-PEG2000), and cholesterol lipids were purchased from Avanti Lipids (Alabaster, AL). 4-(dimethylamino)-butanoic acid, (10Z,13Z)-1-(9Z,12Z)-9,12-octadecadien-1-yl-10,13-nonadecadien-1-yl ester (DLin-MC3-DMA) was purchased from Cayman Chemicals (Ann Arbor, MI). 3,3-Dihexadecyloxycarbocyanine perchlorate (DiO) was purchased from AAT Bioquest (Sunnyvale, CA). Slide-A-Lyzer™ Dialysis Cassettes, gamma-irradiated, 10K MWCO, 0.5 mL were purchased from ThermoFisher Scientific (Waltham, MA). Nanosep® Centrifugal Devices with Omega™ Membrane 10K were purchased from Pall Corporation (Port Washington, NY). An iScript™ cDNA Synthesis kit for RT and 2x SYBR Green Solution for qPCR were purchased from BioRad Technologies (Hercules, CA). Primary monoclonal antibodies were purchased from Cell Signaling Technologies, Inc. (Massachusetts, USA) for Nrf2 (D1Z9C) and GAPDH (14C10) while a beta-actin primary antibody was purchased from Abcam (Cambridge, UK). Secondary antibodies including anti-mouse IgG, HRP-linked Antibody (7076) and anti-rabbit IgG, HRP-linked Antibody (7074) were also purchased from CST. Iscove's Modified Dulbecco's Medium and Dulbecco's Modified Eagle Medium were purchased from ThermoFisher Scientific (Waltham, MA). Citrate buffer was prepared through addition of 255.94 mg of Sodium Citrate dihydrate

and 217 mg of Citric Acid to 20 mL of RNase-free H<sub>2</sub>O. NaOH was added until the solution reached pH = 4.5.

### ***Cell Lines***

Low passage KG-1 and MV4-11 AML cell lines were graciously provided by Dr. Claxton at Penn State. HEK293 cells were donated by Luke Vass and Dr. Kalleth Danappa Jayappa. Human embryonic kidney (HEK293) cells were cultured in Dulbecco's Modified Eagle Medium (DMEM) supplemented with 5% FBS. KG1 and MV4-11 AML cell lines were cultured in Iscove's Modified Dulbecco's Medium (IMDM) supplemented with 5% FBS.

### ***siRNA Design***

Custom siRNA constructs were prepared for Nrf2 and GAPDH. Briefly, gene coding sequences were identified on Ensembl (Hinxton, United Kingdom) and highly conserved exon sequences were moved to Benchling (California, USA) for further analysis. Sequences were analyzed using the ViennaRNA Package in Benchling for theorized free energies of homodimerization and heterodimerization. Sequences were then tested for similarity to other sequences throughout the human genome using a BLAST (NIH) nucleotide → nucleotide search.

### ***siRNA-LNP Formulation***

Lipid nanoparticles were formulated using the NanoAssemblr® Benchtop from Precision NanoSystems Inc. (Vancouver, BC, Canada). All lyophilized siRNA constructs were reconstituted in RNase-free-water to a concentration of 1 mg/mL and then diluted in sterilized citrate buffer (pH = 4.5) to a final concentration of 0.08345 mg/mL. All lipids were dissolved in ethanol at an optimized 10:50:1.5:37.5:1 molar ratio of DSPC, DLin-MC3-DMA, DMG-PEG2000, Cholesterol, and DiO, respectively. The final lipid concentration was diluted to 1.75 mg/mL or 3 mM to achieve an N/P ratio of 2. For microfluidic mixing, total flow rate was set to 12ml/min, with an siRNA to lipid (aqueous to organic) flow ratio of 3:1. Initial and final waste volumes were set to 0.25 and 0.05 mL respectively with a total volume of 0.8 mL. Particle size and zeta potential measurements were conducted through use of a Malvern Zetasizer Nano ZS90 (Malvern, Worcestershire, UK).

### ***Particle Post-Processing***

Following particle formulation, samples were either subject to dialysis or centrifugation. For dialysis, Slide-A-Lyzer™ Dialysis Cassettes were first equilibrated in 1X

PBS solution (pH = 7.4) for two minutes. Samples were then loaded into each cassette and left floating in 250 mL PBS solution under low stirring for two hours at RT. For centrifugation, samples were loaded into a Pall centrifuge filter and centrifuged at 4C for 45 minutes at 2500 g.

### ***In Vitro Transfection***

Cells were plated in 6-well plates at a density of 400,000 cells per well and incubated at 37C for 24 hours prior to transfection. Wells were then treated with either scramble siRNA-LNPs as a control or anti-Nrf2 siRNA in IMDM media at an siRNA dose concentration of 50 nM to 250 nM. Samples were imaged using a 20X objective under white light to see viable cells. Samples were also visualized for the DiO lipid dye using a halogen lamp and green filter.

### ***RT-qPCR***

Sample mRNA was extracted using a trizol based method. Samples were incubated with 1 mL trizol for 5 minutes and then 200 uL of chloroform was added to each tube. After vortexing each sample for 2 minutes, tubes were centrifuged at 4C for 15 minutes at 12k x g. The supernatant of each tube was recovered (roughly 400 uL each) into a new tube and diluted in 500 uL isopropanol. Samples were again vortexed and centrifuged at 4C for 10 minutes at 12k x g. The supernatant was discarded and 1 mL of 75% Ethanol was added to each tube. For a final time, samples were vortexed and centrifuged at 4C for 5 minutes at 7.5k x g. The supernatant was aspirated off each sample and the resulting pellet was resuspended in 30 uL H<sub>2</sub>O. 1 uL of each sample was loaded into a RT tube with other components per the BioRad instructions for RT. After RT, 1 ug of cDNA was added to each well of a 96 well plate along with all other necessary components included in the BioRad protocol for PCR. Each test was run in triplicate. A 52.5C annealing temperature was used based on primer melting temperatures above 55C.

### ***Western Blotting***

Cell samples from 6-well plates were rehydrated with 100 uL of a buffer containing Tris-HCl, SDS, glycerol, and a lysing agent. Samples were sonicated for 12 total seconds with 4 second pulses and 2 second break intervals at 35% amplitude. Samples are then centrifuged for 10 minutes at 4C at 12k x g. Samples were then imaged for protein density using a BCA analysis. Briefly, a 0, 2, 4, 6, 8, and 10 uL BCA (2mg/mL) reagent standard curve was established (diluted in buffer used above and B, A, and S buffers). Protein sample absorbances were then visualized using a Cytation

3 plate reader. 30 ug of protein sample was added to a tube and brought to a total of 50 uL using a buffer containing bromoethanol blue and beta mercaptoethanol. 40 uL of samples were then loaded into a precast 10-15% acrylimide gel and inserted into a BioRad cassette filled with running buffer along with an appropriate DNA ladder (max 250 kDa). Electrodes were attached and a 100 V field was applied to the gel (visualizing bubble accumulation near bottom demonstrates a correct phenomenon) for 1 hour. The gel was placed into the UV chamber and calibrated for total protein using lysine residue excitation. Gels were washed in running buffer on a rocker for 10 minutes while ion pads were soaked in 3:1:1 H<sub>2</sub>O:Methanol:Teabow's transfer Buffer and membranes were soaked in 100% Methanol. Gels were then loaded into a membrane sandwich with (from bottom to top) buffer pads || the gel || PVDF membrane || buffer pads and placed into a transfer system for 15 minutes at a vendor specified voltage. The membrane was then checked for total protein in the UV chamber again using lysine quantification. The membrane was placed into a rocker at room temperature with 20 mL of blocking 5% BSA solution for 30 minutes. The membrane was then washed with TBST buffer to remove excess blocking reagent 3 times. Primary antibody solutions were prepared at 1:1000 concentrations in 5% BSA solution. The gel was cut based on ladder sizes into 3 sections to incubate NRF2, GAPDH, and beta-actin protein samples separately. 5 mL of each primary antibody solution was added to each membrane slice and left on a rocker at 4C overnight (roughly 18 hours). The membrane was washed with TBST buffer 3 times, rocking the sample for 5 minutes upon each rinse. All samples were then treated with either anti-rabbit or ant-mouse HRP solutions at a concentration of 1.2:1000, Ab:5% BSA solution and placed on a rocker at 4C for 1 hour. Gels were then visualized in the UV chamber with a working height of 419 and contrast of 52. Densitometry calculations were conducted in ImageJ.

### ***Combinatorial Treatment***

KG-1 and MV4-11 cell lines were plated at 15,000 cells/well in a 96 well plate. Cells were either treated with 100 nM scramble siRNA LNPs as a control, 100 nM anti-Nrf2 LNPs, 2.5 uM cytarabine, or 100 nM anti-Nrf2 LNPs with 2.5 uM cytarabine. Experimental groups involving LNPs were treated for 24 hours. Following this time for transfection, certain experimental groups were treated with cytarabine. Cell viability was then assessed 4 days following the initial transfection using an MTS assay.

Briefly, 20 uL of a 1000:25 v/v MTS:PES solution was added to each well and left to incubate at 37C for 2 hours. The absorbance of each well at 490 nm was quantified using a Cytation3 plate reader.

## **Results**

### ***Anti-Nrf2 siRNA Design***

An siRNA construct targeting exon 5 of the most common Nrf2 mRNA isoform was validated to have low predicted off-target binding. Particularly, the ViennaRNA algorithm predicted a -2.8 kcal free energy of homodimerization and no thermodynamically favorable binding events between separate siRNA molecules. A BLAST search also vindicated the projected specificity with the closest sequence homology occurring with a proprotein convertase subtilisin/kexin type 5 enzyme achieving only 68% query cover. The construct is therefore expected to selectively bind the Nrf2 locus in future experimentation.

### ***Optimized Particle Formulation***

LNP formulations exhibited high polydispersity with a peak on the order of microns when immediately characterized following formulation (Figure 1A). Post-processing of particles was conducted to remove free siRNA or lipids as well as perform buffer exchange from cytotoxic ethanol to physiologically inert PBS. Particle dialysis led to a highly monodispersed particle population with an average diameter of 117 nm and an average zeta potential of -11.3 mV (Figure 1B and 1D). Centrifugation was also performed on LNP formulations but increased particle size dispersity (Figure C).

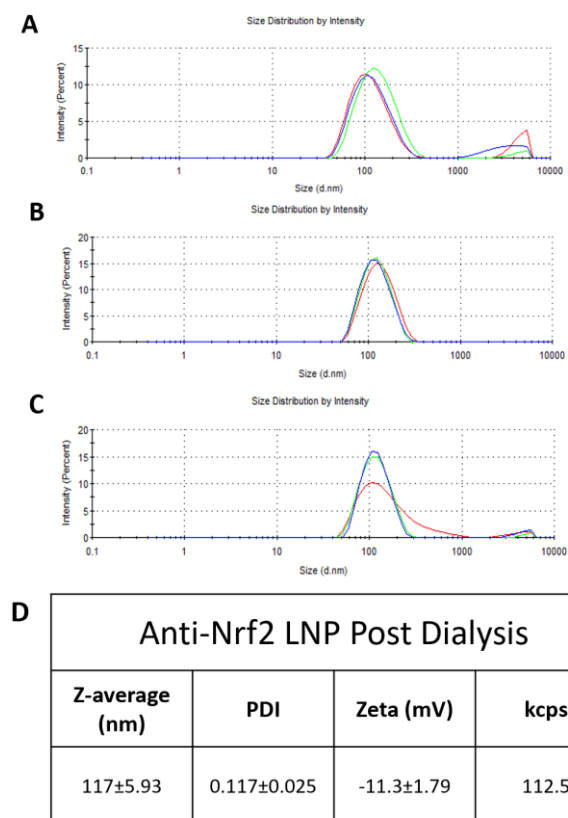


**Figure 1. Effect of post-processing techniques on siRNA-LNP monodispersity.** DLS results are visualized for anti-Nrf2 siRNA loaded LNPs immediately following microfluidic formulation (A) and then either following dialysis against PBS (B) or through centrifugation (C). Each run is processed in triplicate as indicated by multiple color curve lines. Quantitative characterization results (D) are presented for post dialysis particles.

### Transfection of Suspension Cell Lines

The efficiency of LNP transfection of AML cell lines was vindicated through DiO lipid dye imaging. Both KG-1 and MV4-11 cell lines exhibited minimal levels of autofluorescence as indicated by microscopy images of untreated samples (Figure 2A and 2B). However, samples treated with LNPs for 24 hours exhibited high cell specific green signals (Figure 2A and 2B). These signals most likely correspond to DiO residues which suggests successful AML cell internalization of LNPs. HEK293 cells (positive control) exhibited similar DiO signals and inferred LNP uptake (data not shown).

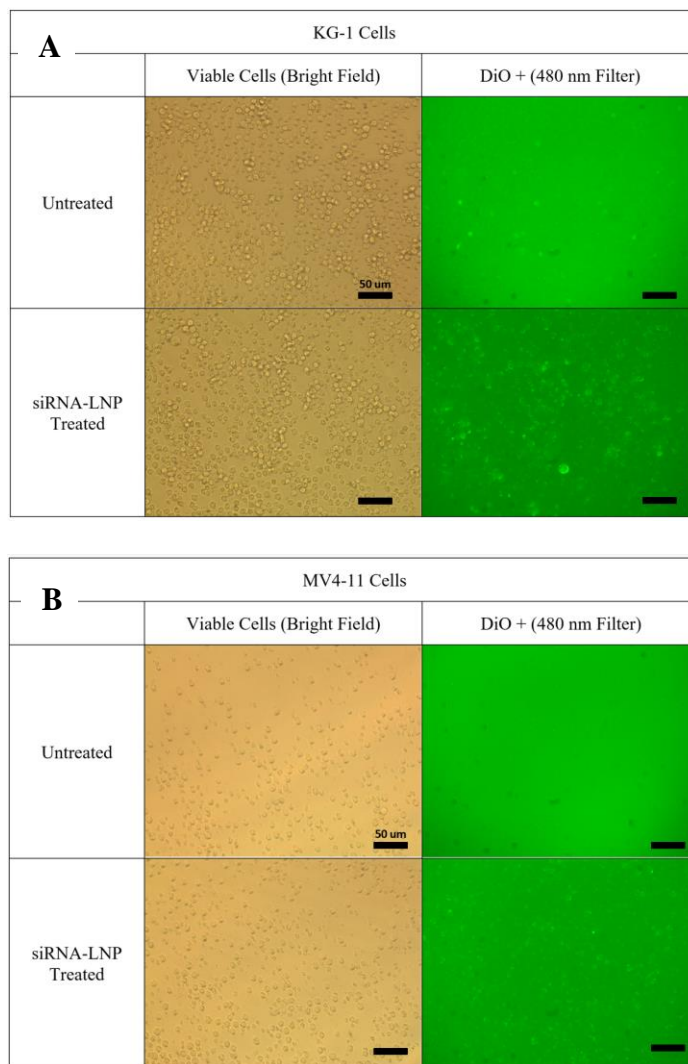


**Figure 2. KG-1 and MV4-11 cells uptake LNPs.** Bright field (left) and 480 nm filtered mercury laser images (right) are shown for KG-1 (A) and MV4-11 (B) cells. Images were taken using auto contrast imaging and a 20X objective lens with a mercury lamp following 24 hours of incubation (37 C and 5% CO<sub>2</sub>). Scale bar represents 50 um.

### Nrf2 Knockdown

Knockdown of Nrf2 mRNA was validated through RT-qPCR. This experiment was tested with a scramble siRNA LNP treatment as a control and an anti-Nrf2 LNP treatment group. A one-way Welch's ANOVA determined significant differences between relative mean Nrf2 mRNA amounts in all treatment groups ( $p = 0.0461$ ). A post-hoc unpaired Welch's t-test vindicated a significant, 2.51-fold knockdown in KG-1 Nrf2 siRNA-LNP treated cells compared to scrambled siRNA control LNPs ( $p = 0.0177$ ).

Anti-Nrf2 LNP treatment also led to reduced relative Nrf2 mRNA in MV4-11 cells though this difference was not significant. Nrf2 protein bands were not observed through western blotting due to probe related defects so conclusions concerning knockdown were only made at the mRNA level. Treatment of MV4-11 cells with anti-GAPDH siRNA LNPs led to noticeable knockdown of GAPDH protein (data not shown). These findings demonstrate the versatility of siRNA LNP vectors in transfection of suspension AML cell lines.

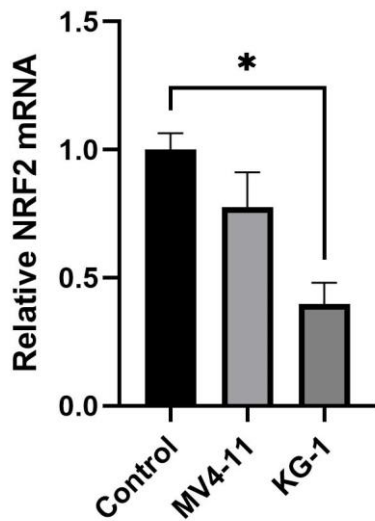


**Figure 3. Knockdown of Nrf2 in MV4-11s through siRNA-LNP based transfection.** RNA was extracted from AML cells transduced with Nrf2-targeted or scramble siRNA LNP constructs and examined for Nrf2 mRNA expression through RT-qPCR. mRNA expression was normalized to GAPDH mRNA levels. Each sample was processed in triplicate. A statistically significant relative Nrf2 mRNA difference is signified by an asterisk as validated through a Welch’s t-test.

**Combinatorial Treatment Efficacy**

Following positive results of LNP uptake and Nrf2 knockdown, the LNP vector was tested in combination with cytarabine to determine the efficacy a novel treatment. KG1 and MV4-11 cell lines were exposed to four different treatments over a 4 day window. All LNP treatments were conducted at or below 100 nM siRNA concentrations and cytarabine treatments were conducted at 2.5 uM. Both scramble and anti-Nrf2 siRNA LNP treatments yielded similar cell viability indicating minimal

toxicity of LNP vectors (Figure 4). Treatment with cytarabine by itself and in the presence of anti-Nrf2 LNPs both led to noticeable decreases in cell viability though future studies will need to corroborate these findings to understand the true effect size (Figure 4).

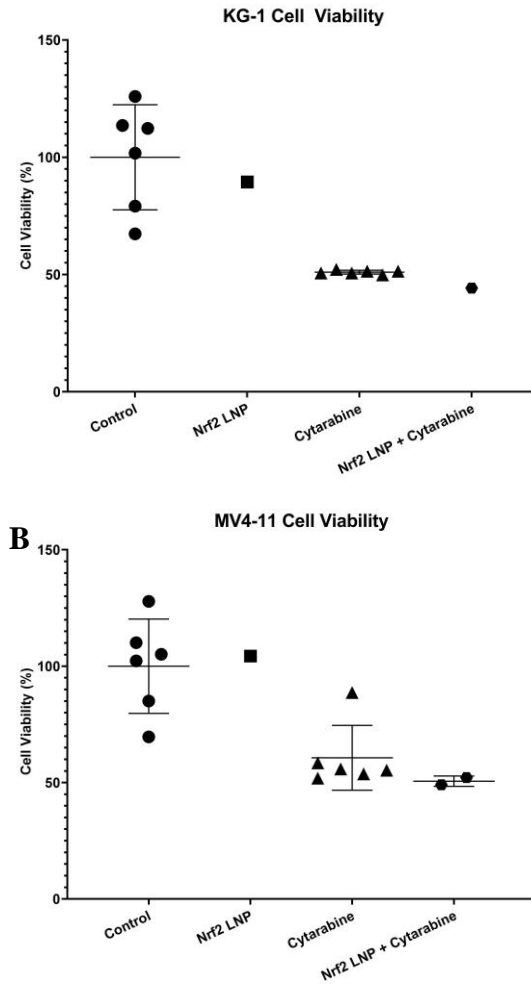


**Figure 4. Therapeutic efficacy of combinatorial treatment including anti-Nrf2 siRNA LNPs and cytarabine.** Cell viability is measured in scramble siRNA LNP treated (Control), anti-Nrf2 siRNA LNP treated (Nrf2 LNP), cytarabine treated (Cytarabine), or anti-Nrf2 siRNA LNP and cytarabine treated (Nrf2 LNP + Cytarabine) groups in both KG-1 (A) and MV4-11 (B) AML cell lines. Percent cell viability is calculated as output MTS assay absorbance value divided by the average absorbance of control samples.



## **Conclusions**

### ***Conclusion***

Presented findings have discovered the successful formulation of scalable, monodispersed anti-Nrf2 siRNA LNPs within functionally viable size range of 117 nanometers following post-processing through dialysis in a physiological buffer. Transfection of KG1 and MV4-11 suspension cell lines with these particles has proven to occur through imaging of excitable lipid components and significant knockdown of Nrf2 mRNA species up to 2.51-fold following RT-qPCR. Preliminary findings have demonstrated the potential therapeutic gain of a combinatorial therapy over the current standard of care though future work must solidify these findings.

### ***Limitations***

The present work utilized only two AML cell lines and one chemotherapy, requiring more iterations with varied experimental groups to truly determine a generalizable claim about therapeutic efficacy. The therapeutic test was also limited by a small sample size leading to the inability for statistical comparisons between treatment groups. This experiment was impacted by bacterial infection in certain treatment wells which reinforces the need for complete sterility in all future experiments. Both the timing and limited supply of Nrf2 siRNA disallowed for the opportunity to replicate these results. Minimal siRNA also limited any ability to test for LNP characterization and transfection at higher titers. This step is imperative in determination of process development for proper manufacturing for clinical translation.

### ***Next Steps***

Future work will primarily determine the true increase in therapeutic efficacy when comparing the standard of care with anti-Nrf2 siRNA LNPs. This process, in addition to earlier transfection and knockdown methods, must also be vindicated in primary harvested AML cell lines. Testing of alternative siRNA designs both within and outside the Nrf2 exon 5 locus or other transcriptional regulators entirely must also be performed. Incorporation of cell specific markers including CD96 or CD117 into LNP formulations will be researched prior to *in vivo* studies for selective treatment of AML cells<sup>19</sup>. In wake of the successes in introducing exogenous siRNA into suspension cell lines, formulation of LNP carriers tuned for plasmid DNA or mRNA payloads may also be examined for treatment of suspension cell-based diseases.

## ***Author Contributions and Notes***

C.C.H. completed the project design and paper writing. The authors declare no conflict of interest.

## ***Acknowledgments***

Dr. Anuradha Illendula assisted with project conception and resource ordering. Dr. Mark Kester provided funding for the work. Luke Vass helped with Western Blotting, RT-qPCR, Experimental Design, and Densitometry Analysis. Dr. Kallesh Danappa Jayappa helped with project conception, siRNA ordering, and provided AML cell line sources. Alex Powell and Eloise Nelson helped with DLS characterization and Cell Culture Maintenance.

## **References**

- (1) Vakiti, A.; Mewawalla, P. Acute Myeloid Leukemia. In *StatPearls*; StatPearls Publishing: Treasure Island (FL), 2021.
- (2) What's New in Acute Myeloid Leukemia (AML) Research? <https://www.cancer.org/cancer/acute-myeloid-leukemia/about/new-research.html> (accessed 2021 -09 -21).
- (3) Thol, F.; Ganser, A. Treatment of Relapsed Acute Myeloid Leukemia. *Curr. Treat. Options Oncol.* **2020**, *21* (8), 66. <https://doi.org/10.1007/s11864-020-00765-5>.
- (4) Koziel, M. J.; Kowalska, K.; Piastowska-Ciesielska, A. W. Nrf2: A Main Responsive Element in Cells to Mycotoxin-Induced Toxicity. *Arch. Toxicol.* **2021**, *95* (5), 1521–1533. <https://doi.org/10.1007/s00204-021-02995-4>.
- (5) Liu, P.; Ma, D.; Wang, P.; Pan, C.; Fang, Q.; Wang, J. Nrf2 Overexpression Increases Risk of High Tumor Mutation Burden in Acute Myeloid Leukemia by Inhibiting MSH2. *Cell Death Dis.* **2021**, *12* (1), 1–15. <https://doi.org/10.1038/s41419-020-03331-x>.
- (6) Sezgin-Bayindir, Z.; Losada-Barreiro, S.; Bravo-Díaz, C.; Sova, M.; Kristl, J.; Saso, L. Nanotechnology-Based Drug Delivery to Improve the Therapeutic Benefits of NRF2 Modulators in Cancer Therapy. *Antioxidants* **2021**, *10* (5), 685. <https://doi.org/10.3390/antiox10050685>.
- (7) Sova, M.; Saso, L. Design and Development of Nrf2 Modulators for Cancer Chemoprevention and Therapy: A Review. *Drug Des. Devel.*

- Ther.* **2018**, *12*, 3181–3197.  
<https://doi.org/10.2147/DDDT.S172612>.
- (8) Saito, T.; Ichimura, Y.; Taguchi, K.; Suzuki, T.; Mizushima, T.; Takagi, K.; Hirose, Y.; Nagahashi, M.; Iso, T.; Fukutomi, T.; Ohishi, M.; Endo, K.; Uemura, T.; Nishito, Y.; Okuda, S.; Obata, M.; Kouno, T.; Imamura, R.; Tada, Y.; Obata, R.; Yasuda, D.; Takahashi, K.; Fujimura, T.; Pi, J.; Lee, M.-S.; Ueno, T.; Ohe, T.; Mashino, T.; Wakai, T.; Kojima, H.; Okabe, T.; Nagano, T.; Motohashi, H.; Waguri, S.; Soga, T.; Yamamoto, M.; Tanaka, K.; Komatsu, M. P62/Sqstm1 Promotes Malignancy of HCV-Positive Hepatocellular Carcinoma through Nrf2-Dependent Metabolic Reprogramming. *Nat. Commun.* **2016**, *7* (1), 12030. <https://doi.org/10.1038/ncomms12030>.
- (9) Rondeau, G.; Abedinpour, P.; Chrastina, A.; Pelayo, J.; Borgstrom, P.; Welsh, J. Differential Gene Expression Induced by Anti-Cancer Agent Plumbagin Is Mediated by Androgen Receptor in Prostate Cancer Cells. *Sci. Rep.* **2018**, *8* (1), 2694. <https://doi.org/10.1038/s41598-018-20451-9>.
- (10) Song, Y.; Yuan, Y.; Shi, X.; Che, Y. Improved Drug Delivery and Anti-Tumor Efficacy of Combinatorial Liposomal Formulation of Genistein and Plumbagin by Targeting Glut1 and Akt3 Proteins in Mice Bearing Prostate Tumor. *Colloids Surf. B Biointerfaces* **2020**, *190*, 110966. <https://doi.org/10.1016/j.colsurfb.2020.110966>.
- (11) He, W.; Bennett, M. J.; Luistro, L.; Carvajal, D.; Nevins, T.; Smith, M.; Tyagi, G.; Cai, J.; Wei, X.; Lin, T.-A.; Heimbrook, D. C.; Packman, K.; Boylan, J. F. Discovery of siRNA Lipid Nanoparticles to Transfect Suspension Leukemia Cells and Provide In Vivo Delivery Capability. *Mol. Ther.* **2014**, *22* (2), 359–370. <https://doi.org/10.1038/mt.2013.210>.
- (12) Adams, D.; Gonzalez-Duarte, A.; O’Riordan, W. D.; Yang, C.-C.; Ueda, M.; Kristen, A. V.; Tournev, I.; Schmidt, H. H.; Coelho, T.; Berk, J. L.; Lin, K.-P.; Vita, G.; Attarian, S.; Planté-Bordeneuve, V.; Mezei, M. M.; Campistol, J. M.; Buades, J.; Ill, T. H. B.; Kim, B. J.; Oh, J.; Parman, Y.; Sekijima, Y.; Hawkins, P. N.; Solomon, S. D.; Polydefkis, M.; Dyck, P. J.; Gandhi, P. J.; Goyal, S.; Chen, J.; Strahs, A. L.; Nochur, S. V.; Sweetser, M. T.; Garg, P. P.; Vaishnav, A. K.; Gollob, J. A.; Suhr, O. B. Patisiran, an RNAi Therapeutic, for Hereditary Transthyretin Amyloidosis. *N. Engl. J. Med.* **2018**. <https://doi.org/10.1056/NEJMoa1716153>.
- (13) Roces, C.; Lou, G.; Jain, N.; Abraham, S.; Thomas, A.; Halbert, G.; Perrie, Y. Manufacturing Considerations for the Development of Lipid Nanoparticles Using Microfluidics. *Pharmaceutics* **2020**, *12*, 1095. <https://doi.org/10.3390/pharmaceutics12111095>.
- (14) Meel, R. van der; Chen, S.; Zaifman, J.; Kulkarni, J. A.; Zhang, X. R. S.; Tam, Y. K.; Bally, M. B.; Schiffelers, R. M.; Ciufolini, M. A.; Cullis, P. R.; Tam, Y. Y. C. *Modular Lipid Nanoparticle Platform Technology for siRNA and Lipophilic Prodrug Delivery*, 2020; p 2020.01.16.907394. <https://doi.org/10.1101/2020.01.16.907394>.
- (15) Kim, M.; Jeong, M.; Hur, S.; Cho, Y.; Park, J.; Jung, H.; Seo, Y.; Woo, H. A.; Nam, K. T.; Lee, K.; Lee, H. Engineered Ionizable Lipid Nanoparticles for Targeted Delivery of RNA Therapeutics into Different Types of Cells in the Liver. *Sci. Adv.* *7* (9), eabf4398. <https://doi.org/10.1126/sciadv.abf4398>.
- (16) Sharma, D.; Maheshwari, D.; Philip, G.; Rana, R.; Bhatia, S.; Singh, M.; Gabrani, R.; Sharma, S. K.; Ali, J.; Sharma, R. K.; Dang, S. Formulation and Optimization of Polymeric Nanoparticles for Intranasal Delivery of Lorazepam Using Box-Behnken Design: In Vitro and In Vivo Evaluation. *BioMed Res. Int.* **2014**, *2014*, 156010. <https://doi.org/10.1155/2014/156010>.
- (17) Mihaila, R.; Chang, S.; Wei, A. T.; Hu, Z. Y.; Ruhela, D.; Shadel, T. R.; Duenwald, S.; Payson, E.; Cunningham, J. J.; Kuklin, N.; Mathre, D. J. Lipid Nanoparticle Purification by Spin Centrifugation–Dialysis (SCD): A Facile and High-Throughput Approach for Small Scale Preparation of siRNA–Lipid Complexes. *Int. J. Pharm.* **2011**, *420* (1), 118–121. <https://doi.org/10.1016/j.ijpharm.2011.08.017>.
- (18) Rushworth, S. A.; Zaitseva, L.; Murray, M. Y.; Shah, N. M.; Bowles, K. M.; MacEwan, D. J. The High Nrf2 Expression in Human Acute Myeloid Leukemia Is Driven by NF-κB and Underlies Its Chemo-Resistance. *Blood* **2012**, *120* (26), 5188–5198. <https://doi.org/10.1182/blood-2012-04-422121>.

- (19) Hosen, N.; Park, C. Y.; Tatsumi, N.; Oji, Y.; Sugiyama, H.; Gramatzki, M.; Krensky, A. M.; Weissman, I. L. CD96 Is a Leukemic Stem Cell-Specific Marker in Human Acute Myeloid Leukemia. *Proc. Natl. Acad. Sci. U. S. A.* **2007**, *104* (26), 11008–11013.  
<https://doi.org/10.1073/pnas.0704271104>.